CHAPTER FIVE
FINITE ELEMENT MODELING

5.1 General

To study the behavior of NSRPC beams of the present research theoretically, numerical method was adopted and represented through finite element analysis. The theoretical analysis was performed by using the finite element models in the finite element package ANSYS[79].

The accuracy and validity of the adopted finite element procedure are checked and verified in this chapter by comparison of the ANSYS output with the experimental results. The beneficial effects of using nanosilica and fiber reinforcement to strengthen and increase the shear capacity of beams are very well assured and confirmed by such comparison. The accuracy of the finite element models was determined by ensuring that the ultimate load, deflection, cracks propagation and applied theory of failure were reasonably predicted with the overall structural response and load-deflection behavior were found in reasonable agreement with the experimental test results.

The material properties throughout simulation using finite elements approach and the governing constitutive relationships are considered over these elements and expressed in terms of unknown values at element corners. An assembly process results in a set of equations. Solution of these equations gives the approximate behavior of the models.

5.2 Finite Element Modeling

Reinforced concrete beams "RCB" were modeled by selecting a suitable element that simulates the reality and this phenomenon was adopted for all structural and materials elements. For concrete element, the model is capable of predicting failure for concrete materials. Both cracking and crushing failure modes are accounted for. The two input strength parameters, ultimate uniaxial tensile and compressive strengths, are needed to define a failure surface for the concrete. Modeling of main steel reinforcement for main and stirrups was discrete representation. Discrete representation has been widely used. The reinforcement in the discrete model used one dimensional bar elements that are connected to concrete mesh nodes. Therefore, the concrete and the reinforcement mesh share the same nodes and the same occupied regions. Full displacement compatibility between the reinforcement and concrete is a significant advantage of the discrete representation. Their disadvantages are the restriction of the mesh and the increase in the total number of elements.

5.3 Assumptions

The assumptions made in the static analysis are summarized below:

1- Concrete and steel were modeled as isotropic and homogeneous materials.

2- Steel was assumed to be an elastic-perfectly plastic material and identical in tension and compression.

3- Initially plane sections remain plane after loading that is, the strain in the concrete and the reinforcement is proportional to the distance from the neutral axis.

4- The maximum compressive strain in the concrete is assumed to be 0.005 mm/mm.

5- Perfect bond exits between different materials.

6- Self-weight of the beams was ignored.

7- Additives materials distributed uniformly through concrete.

5.4 Element Types

The elements types shown in Table 5.1 were used to simulate all model tested beams.

Table 5.1 Element Types [79]

Element No.	Element type	Representation
1	SOLID65	Concrete cross section.
2	LINK8	Longitudinal Steel reinforcement top and bottom.
3	LINK8	Stirrups.
4	SOLID 45	Support.

5.4.1 SOLID65 Element

SOLID65 element is used for the 3-D modeling of solids with or without reinforcing bars. SOLID65 element is capable of representing the cracking in tension and crushing in compression. The element shown in Fig. 5.1 is defined by eight nodes having three degrees of freedom at each node, translations in the nodal x, y, and z directions.

The most important aspect of this element is treatment of nonlinear material properties. The concrete model is capable to provide of cracking in three orthogonal directions, crushing, plastic deformation, and creep. The rebars are providing of tension and compression, but not shear. They are also capable to provide of plastic deformation and creep. This element was used to model the concrete.

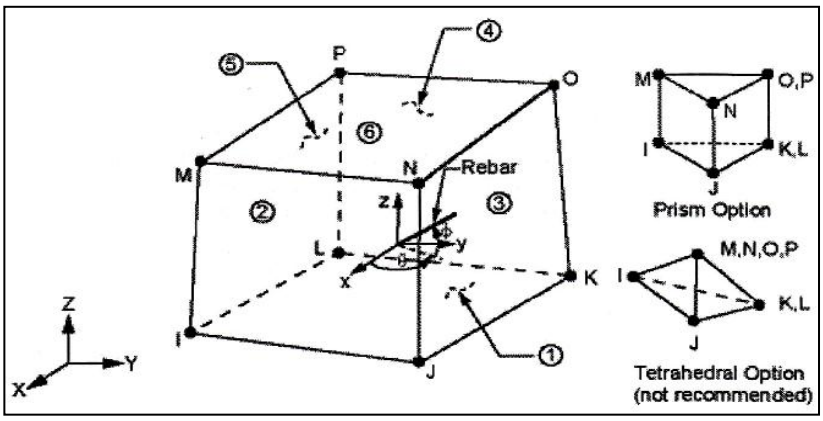

Fig. 5.1 SOLID65 Element Geometry.

5.4.2 LINK8 Element

This element can be used to model main and stirrups reinforcement. The 3-D spar element is a uniaxial tension-compression element with three degrees of freedom at each node, translations in the nodal x, y, and z directions, no bending of the element is considered. Plasticity, creep, swelling, stress stiffening, and large deflection capabilities are included. Fig. 5.2 shows the geometry of link8 element.

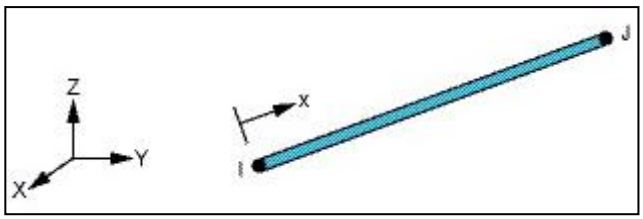

Fig. 5.2 LINK8 Geometry.

5.4.3 SOLID45 Element

SOLID45 is used for the three-dimensional modeling of solid structures(Fig.5.3). The element is defined by eight nodes having three degrees of freedom at each node: translations in the nodal x, y, and z directions. The element has plasticity, creep, swelling, stress stiffening,

large deflection, and large strain capabilities. This type of element was used to simulate plates placed at top of tested beam under the applied loading and also to simulate supports. No real constant is needed for this type of element.

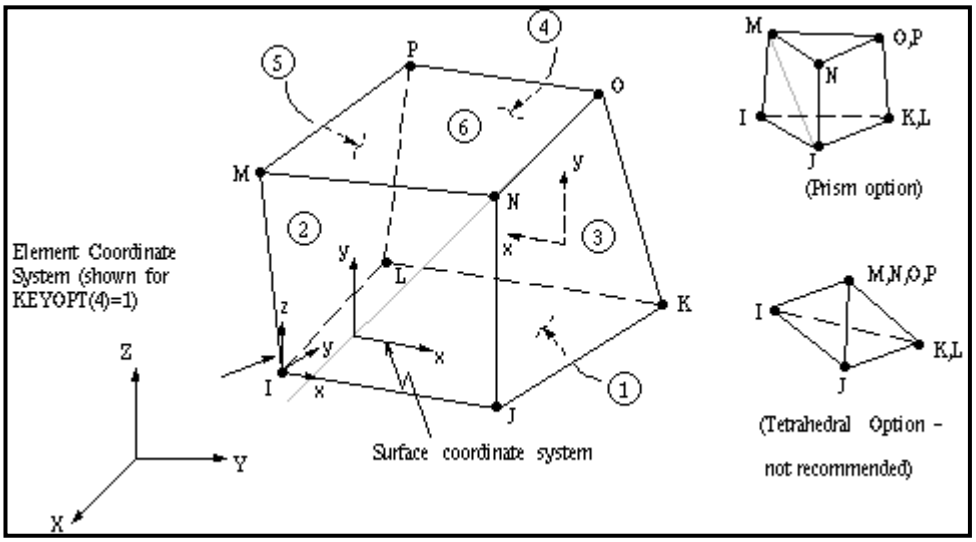

Fig. 5.3: SOLID45 Geometry.

5.5 Real Constant

The real constant for SOLID65 element requires information about smeared reinforcement in three directions x, y and z, volume ratio and orientation angle. In the present research, discrete representation of steel reinforcement was adopted, but fiber reinforcement was inserted as a new material mixed with cement mortar for different volume percentages. Therefore, all real constants for SOLID65 element were equal to specified fiber reinforcement in three directions according to the orientation. Also that for Nano material was added to the solid65 as function of compressive strength , tensile strength and modulus of elasticity.

The real constant for LINK8 requires information about the cross sectional area of the reinforcing bars are shown in Table 5.2.

Table 5.2 Real Constant for Model Beam

Real Constant Set	Element Type	Constant				
1	SOLID 65	Real Constant for Steel Fibers	Volume Ratio	Orientation Angle		
		1	0%	0	90	90
				90	0	90
				90	90	0
		2	1%	0	90	90
				90	0	90
				90	90	0
		3	2%	0	90	90
				90	0	90
				90	90	0
2	LINK 8	Cross-sectional area mm^2	According to steel ratio			
		Initial strain mm/mm	0			
3	LINK 8	Cross-sectional area mm^2	29			
		Initial strain mm/mm	0			

5.6 Material Properties

Material numbers "1" represent the concrete beam. This element requires linear isotropic material properties to properly model the concrete. Modulus of elasticity, compressive strength of concrete and tensile strength as actual values from tests were used. Poisson's ratio for concrete was assumed to be 0.15 for all beams. Concrete material data such as the shear transfer coefficients, tensile strength, and compressive strength are described in Table 5.3.

Table 5.3 SOLID65 Concrete Material Data

Constant	Meaning
1	Shear transfer coefficients for an open crack, β_o.
2	Shear transfer coefficients for a closed crack, β_c.
3	Uniaxial tensile cracking stress.
4	Uniaxial crushing stress positive.
5	Biaxial crushing stress positive.
6	Ambient hydrostatic stress state for use with constants 7 and 8.
7	Biaxial crushing stress positive under the ambient hydrostatic stress state constant 6.
8	Uniaxial crushing stress positive under the ambient hydrostatic stress state constant 6.
9	Stiffness multiplier for cracked tensile condition.

Typical shear transfer coefficients range from 0 to 1, with 0 representing a smooth crack with complete loss of shear transfer and 1 representing a rough crack with no loss of shear transfer. The coefficient for open crack was set to 0.2, while the coefficient for closed crack was

set to 0.7. These values are suitable and recommended by many researchers. Material numbers 2 and 3 refer to LINK8 element which represent longitudinal steel reinforcement and stirrups respectively, and this element is assumed to be linear isotropic. Material number 4 refers to SOLID 45 which is used to simulate supports and plates under applied loading.

5.7 Modeling

NSRPC beams were modeled as prismatic beams as shown in Fig. 5.4. The beam dimensions adopted in the present study were analyzed and designed according to ACI – 318 – 2011 [80] .

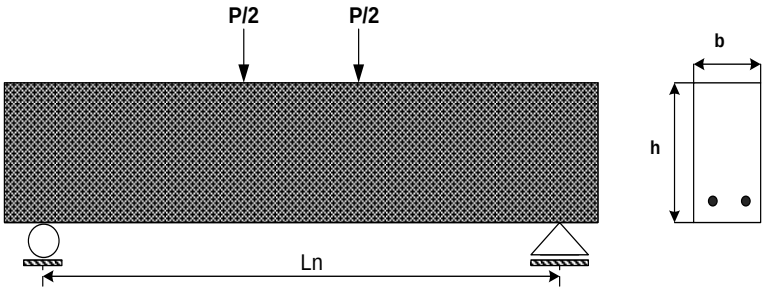

Fig. 5.4 NSRPC Beam

The nonlinear performance of steel was assumed to be linear – perfectly plastic as shown in Fig. 5.5. Nonlinearity of concrete represented by its compressive stress-strain curves depends on the mix type and the type of additive materials. Fig. 5.6 shows the effect of NS on compressive stress-strain curves, while Figs. 5.6 to 5.9 show respectively the effects of SF, Vf and absence of NS and Vf on compressive stress-strain curves.

In the application of finite element approach to nonlinear analysis, one has to update the stiffness matrix constantly in order to take account of the nonlinear effects that are present. The equilibrium configuration of

the structure changes constantly, so those in present studies carry out the analysis in a series of load increments. The equilibrium and kinematic state of the structure at the end of the one load increment are used to formulate the stiffness relationship for the solution of the next load increment. Displacement control method was adopted to reach the ultimate loading applied in experimental tests. In the present study ,nonlinear finite element analysis was used , the load was applied in increments and the nonlinear problem was solved by a series of linearized steps. The stiffness matrix relating the incremental force vector with the incremental displacement vector was referred to as the incremental stiffness matrix. Newton-Raphson numerical method was adopted with accuracy 0.001 to solve the incremental loading steps. The maximum 150 load steps applied was used to reach the final solution and final results tests.

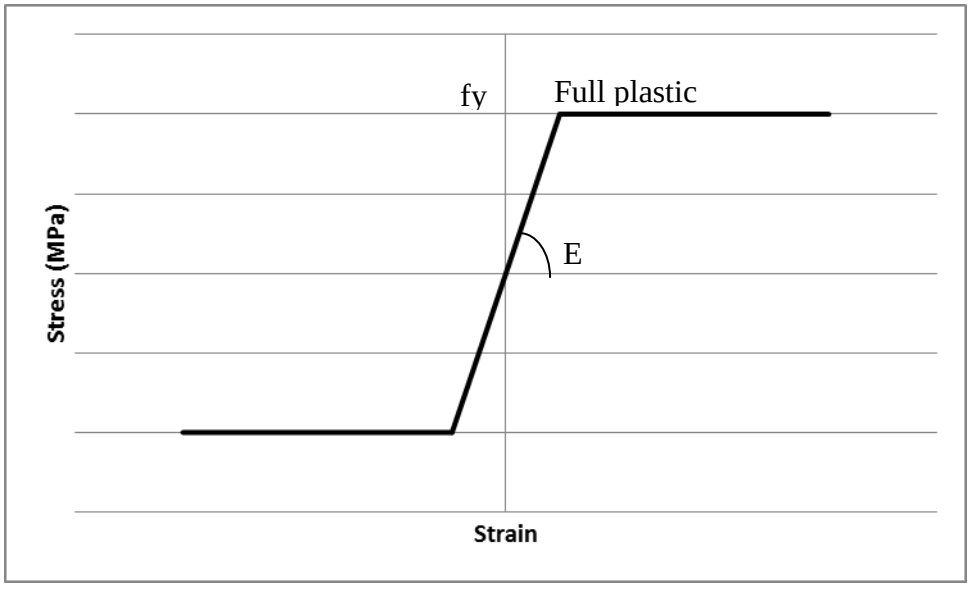

Fig. 5.5 Stress-Strain Curve of Steel.

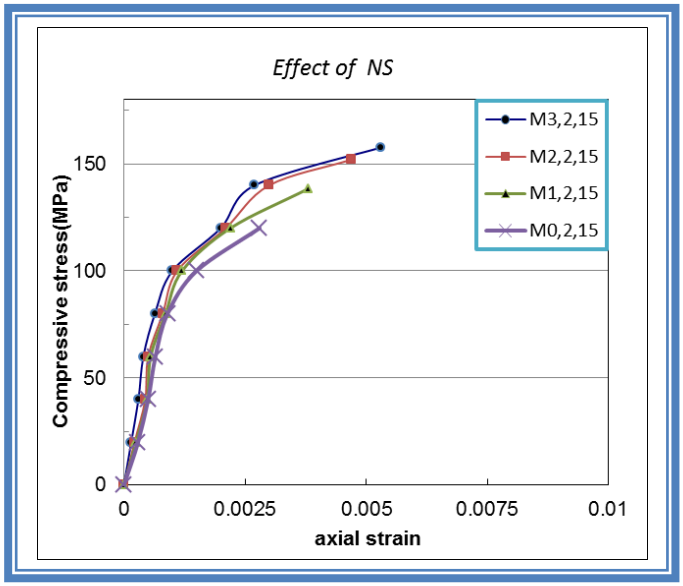

Fig. 5.6: Stress-Strain Curves of NSRPC, NS as a Variable

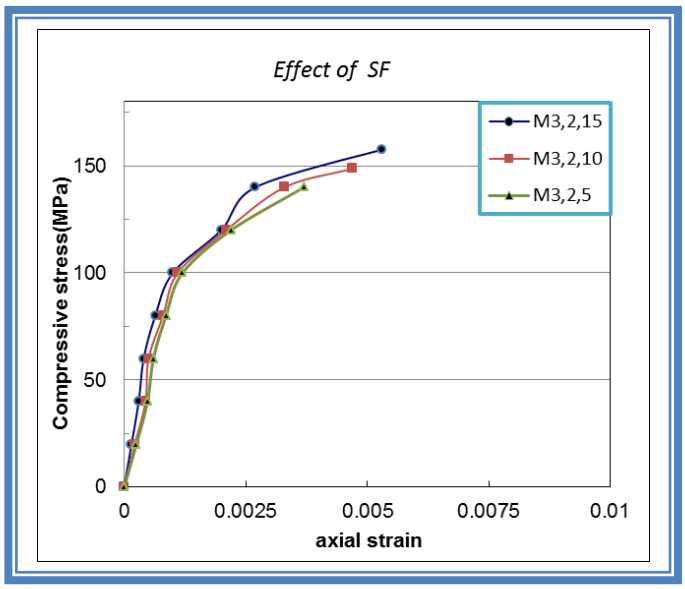

Fig. 5.7: Stress-Strain Curves of NSRPC, SF as a Variable

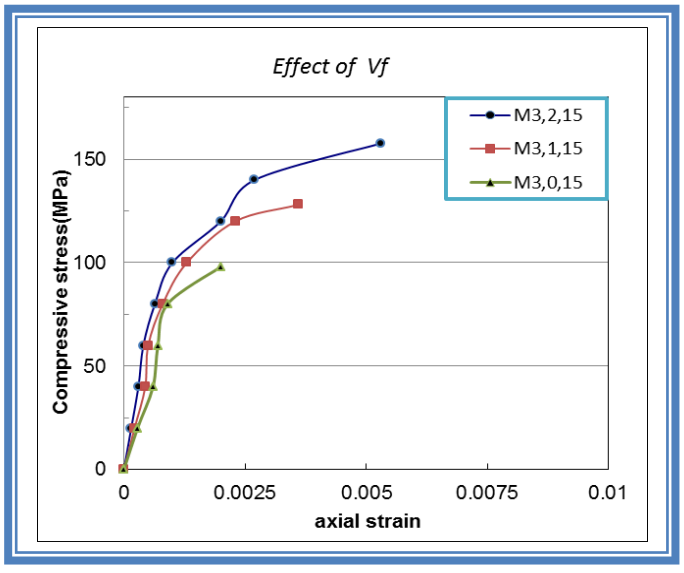

Fig. 5.8: Stress-Strain Curves of NSRPC, Vf as a Variable

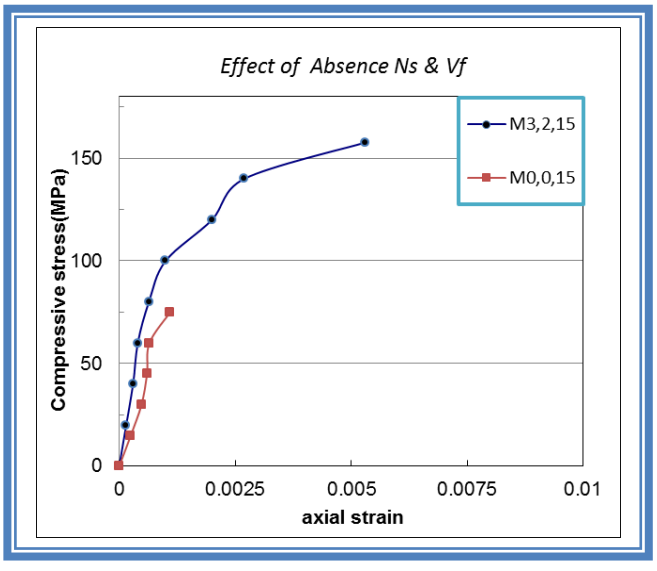

Fig. 5.9: Stress-Strain Curves of NSRPC, with Absence of NS and Vf

5.7.1 Meshing

To obtain good results from the Solid65 element, the use of a cubic mesh with ratio a round unity was adopted. The overall mesh of the finit element model of the beam created in ANSYS is shown in Fig. 5.10**.** No mesh of the reinforcement is needed because individual elements are created in the model through the nodes created by the mesh of the concrete volumes,

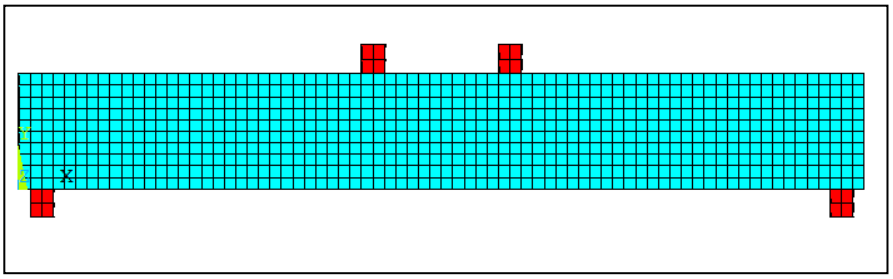

Fig. 5.10 Concrete Solid Meshing.

5.8 Boundary Conditions and Loads

The supports were simulated to match their real form in laboratory. Four points loading was applied similar to the actual experimental loading for each specimen. Since the actual loads were applied on top of steel plates, these plates were simulated by choosing suitable elements with width and thickness identical with those used in laboratory. The application of the loads up to failure was done incrementally as required by the Newton - Raphson procedure. Total applied load was divided into a series of load increments representing the steps. Within each load step, maximum of 150 iterations were permitted with a minimum number of iteration equal to one.

5.9 Results

According to models that simulated using finite elements approach by ANSYS, the following performance was noted.

5.9.1 General performance

The general performance of all models that simulated by ANSYS can be summarized as below:

1. Deflection was nonlinear.
2. Values of deflection greater than ACI Code, maximum allowable limit were obtained.
3. A 45^{o} diagonal crack was formed starting from each support and propagating to top face of beam.
4. Cracks propagated towards top with plastic hinges developed due to increase in loading.
5. There are enhancements in tensile stress of concrete due to the presence of additive materials.
6. Strains in concrete along longitudinal axis at top and bottom faces of the beam mid-span section were greater than their allowable limits.

5.9.2 Deflection

Deflections were evaluated and drawn to check the behavior of RC beams. The central deflection was measured and recorded at every load step which showed nonlinear behavior. Figs. 5.11 to 5.26 show the deflected shapes of all the sixteen NSRPC beams of the present research as predicted by the finite element package ANSYS. The deflected shape of each beam was obtained by applying a series of load increments on the beam in accordance with the beams ultimate load capacity as measured experimentally. According to the specifications given by the ACI code[1] , the maximum allowable deflection for a simply supported beam under service loading should not exceed "L/360". This gives a permissible value of deflection for a 1.4 m span beam as small as 3.9 mm. It can be seen from Figs.(5-27) to (5-43) that within the elastic range of the load-deflection curve, the deflection at center of beam is below the allowable value of 3.9 mm but at ultimate load it is far beyond that. Comparison between the load deflection curves predicted by ANSYS with those obtained experimentally (as shown in Figs. 5-76 to 5-91) indicates that the beam showed a stiffer response in the elastic range according to ANSYS in comparison with the experimental tests. However with continuing deflection and propagation of cracking the reverse behavior was noticed and the slope of the load-deflection curve according to ANSYS was lower than that found experimentally. Comparison between ANSYS results and those found experimentally for the values of deflections obtained at first cracking load and at ultimate load are shown in Tables5.4 and 5.5respectively.

5.9.3 Cracks propagations

Figs. 5.44 to 5.59 show the cracks propagations for each beam model at ultimate load. Each crack represents the average of three cracks (first, second and third cracks) which may form in different directions x ,y and z. The amount and concentration of cracks depend on the magnitude of the applied loading, percentage of fiber reinforcement by weight, percentage of Nano by volume and presence of stirrups. The effect of fiber reinforcement enhanced the behavior of reinforced concrete beams because of its virtue in increasing the resistance capacity of concrete against tensile stress and then reduce cracks. On the other hand , the effect of nanosilica as a material increases the compressive strength of concrete and therefore also helps in reducing the propagation of cracks.

5.9.4 Strain

Figures 5.60 to 5.75 show the ANSYS results of the longitudinal strains along the beam span. There are two zones according to the sign convention, positive tension and negative compression. Because the beam is simply supported the compression is at top and the tension is at bottom. The presence of fiber reinforcement and nanosilica increased the compressive strength of concrete and made the concrete more ductile in tension zone. This enhanced the concrete to resist tensile stresses and eventually reducing the cracks.

Table 5.4 ANSYS Deflections at First cracking Loading Compared with Experimental Results.

Beam	Deflection at first crack load (mm) experimental	Deflection at first crack load (mm) ANSYS	$\frac{\Delta cr_{ANSYS}}{\Delta cr\ exp.}$
B1	3.2	3.2	1
B2	3.6	2.9	0.8
B3	3.5	2.7	0.77
B4	3.6	2.9	0.8
B5	2.8	2.3	0.82
B6	3.0	2.4	0.8
B7	3.6	2.3	0.63
B8	3.4	2.6	0.76
B9	3.7	2.8	0.75
B10	3.8	3.1	0.82
B11	2.3	1.9	0.83
B12	1.5	1.6	1.06
B13	2.7	2.6	0.96
B14	1.9	2.6	1.4
B15	2.8	2.2	0.79
B16	4.5	3.8	0.84

Table 5.5 ANSYS Deflections at Ultimate Load Compared with Experimental Results.

Beam No.	% Fiber Reinforcement	%Nanosilica	Ultimate load, (kN)	Maximum Deflection - Experimental (mm)	Maximum Deflection - ANSYS (mm)	$\frac{\Delta cr_{ANSYS}}{\Delta cr\ exp.}$
B1	2	0	215	14.5	16.04	1.1
B2	2	1	245	13.3	14.92	1.12
B3	2	2	255	12.7	13.84	1.08
B4	2	3	269	12.3	14.38	1.16
B5	2	3	243	13.8	13.21	0.96
B6	2	3	253	13.2	13.83	1.04
B7	0	3	90	5.7	6.42	1.13
B8	1	3	185	9.0	9.83	1.09
B9	2	3	312	11.5	12.81	1.1
B10	2	3	328	10.8	13.50	1.25
B11	2	3	335	12.9	11.55	0.89
B12	2	3	416	13.4	13.10	0.97
B13	1	3	218	10.2	11.20	1.09
B14	1	3	275	11.0	12.60	1.14
B15	0	3	175	9.2	10.00	1.08
B16	0	0	70	6.0	5.44	0.91

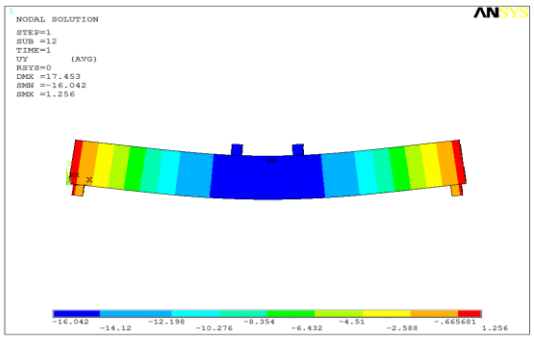

Fig. 5.11 Deflected Shape of Beam (B1)

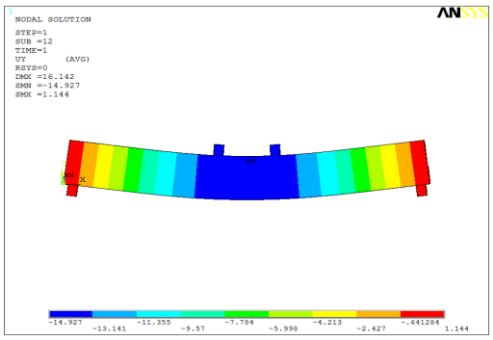

Fig. 5.12 Deflected Shape of Beam (B2)

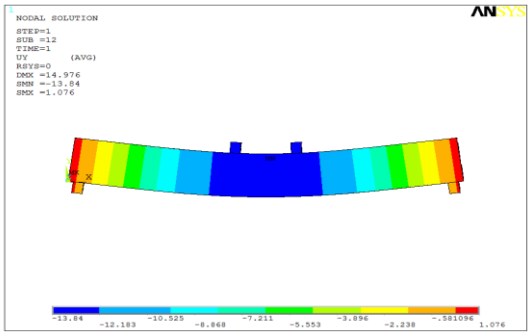

Fig. 5.13 Deflected Shape of Beam (B3)

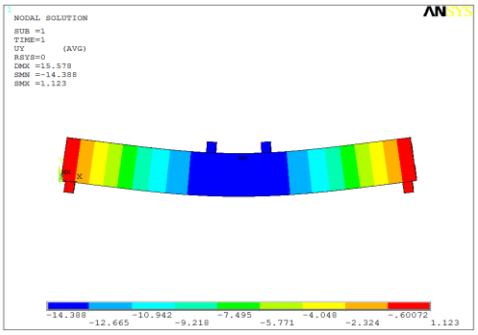

Fig. 5.14 Deflected Shape of Beam (B4)

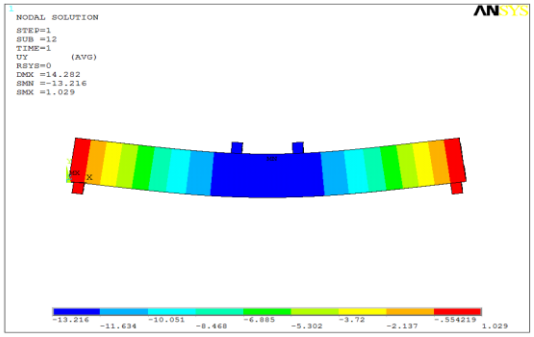

Fig. 5.15 Deflected Shape of Beam (B5)

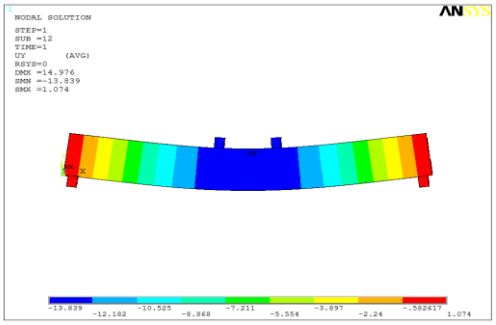

Fig. 5.16 Deflected Shape of Beam (B6)

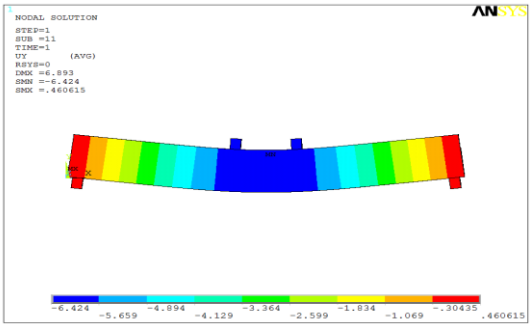

Fig. 5.17 Deflected Shape of Beam (B7)

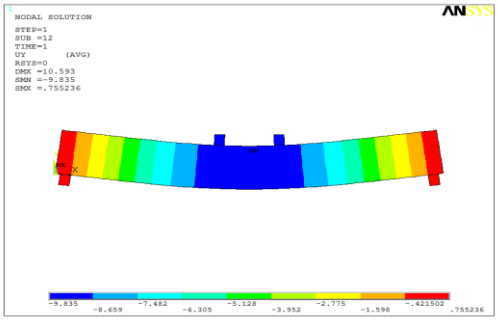

Fig. 5.18 Deflected Shape of Beam (B8)

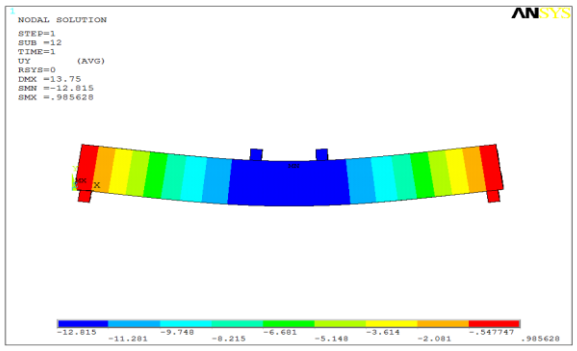

Fig. 5.19 Deflected Shape of Beam (B9)

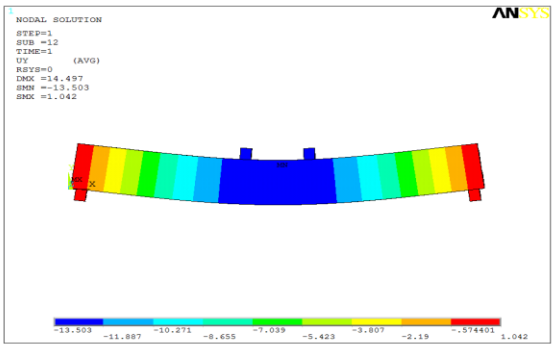

Fig. 5.20 Deflected Shape of Beam (B10)

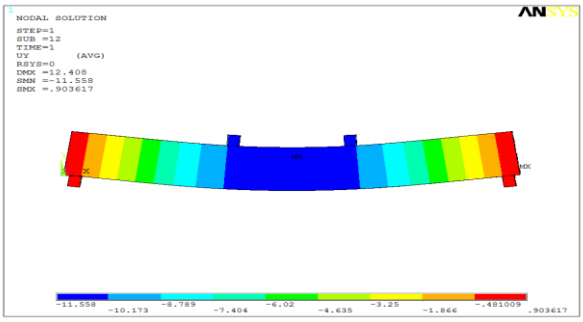

Fig. 5.21 Deflected Shape of Beam (B11)

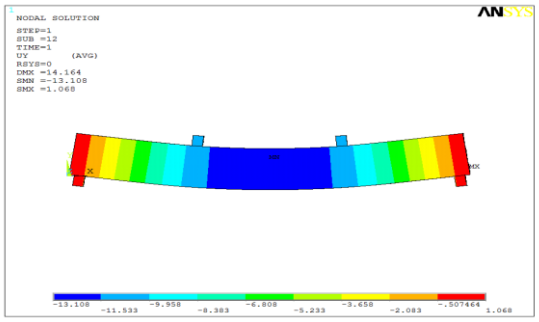

Fig. 5.22 Deflected Shape of Beam (B12)

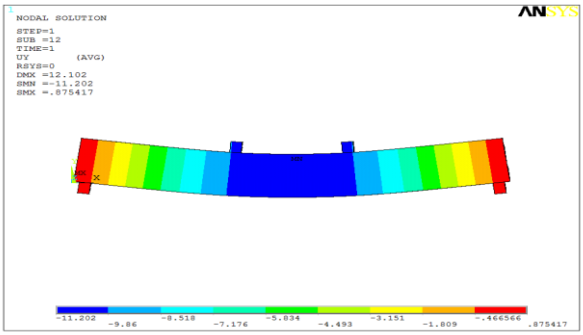

Fig. 5.23 Deflected Shape of Beam (B13)

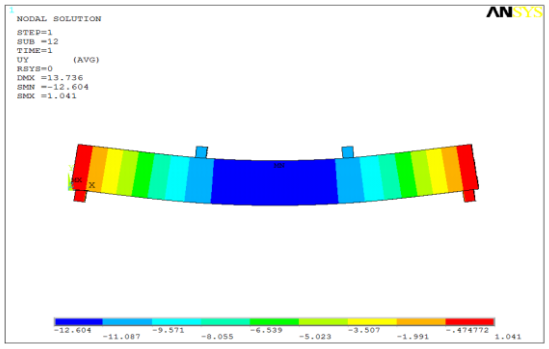

Fig. 5.24 Deflected Shape of Beam (B14)

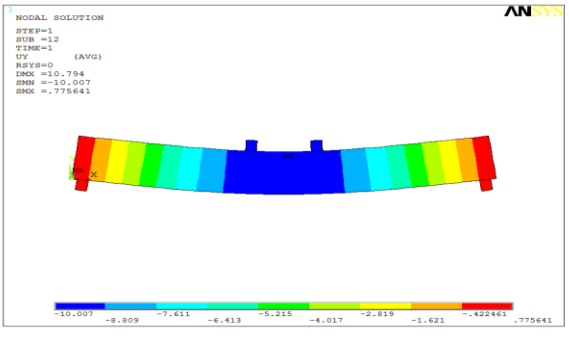

Fig. 5.25Deflected Shape of Beam (B15)

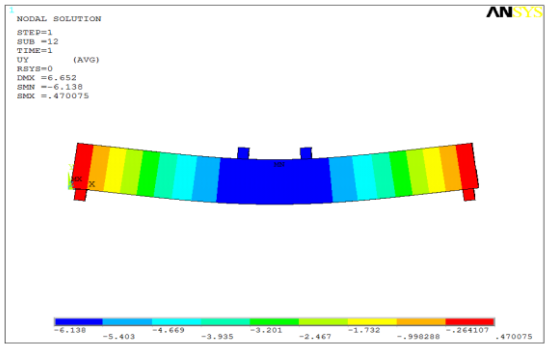

Fig. 5.26 Deflected Shape of Beam (B16)

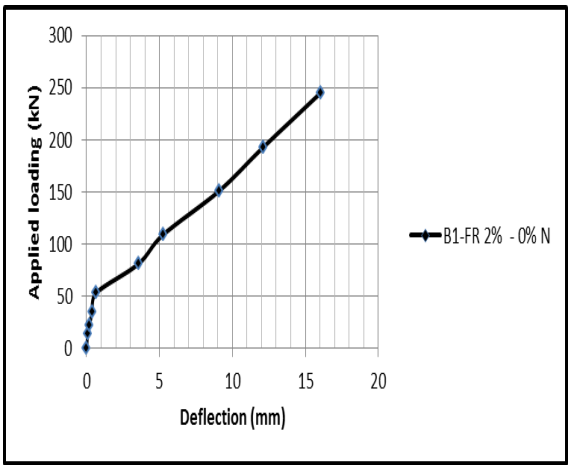

Fig. 5.27 Load – Deflection Curve of Beam (B1).

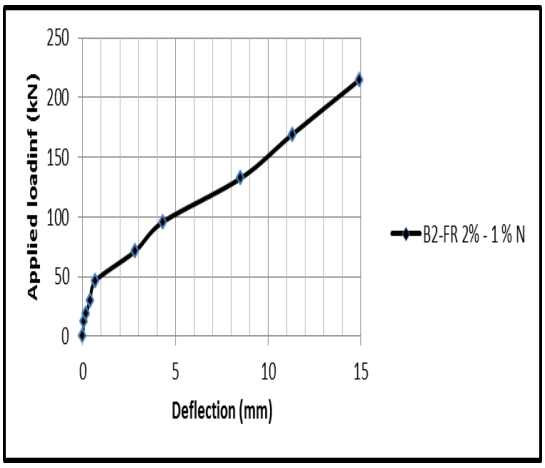

Fig. 5.28 Load – Deflection Curve of Beam (B2).

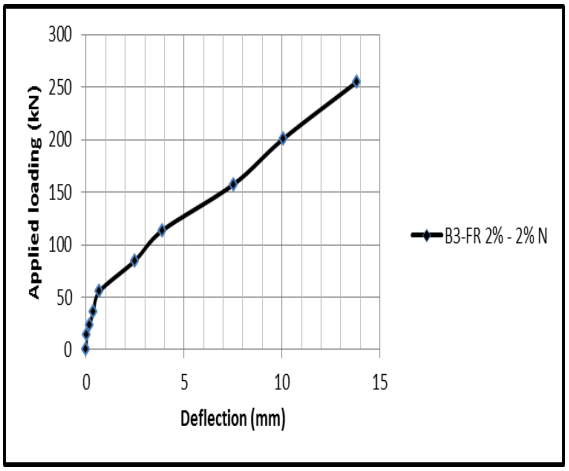

Fig. 5.29 Load – Deflection Curve of Beam (B3).

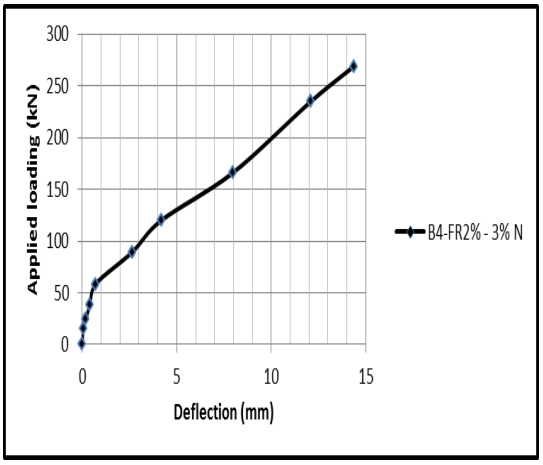

Fig. 5.30Load – Deflection Curve of Beam (B4).

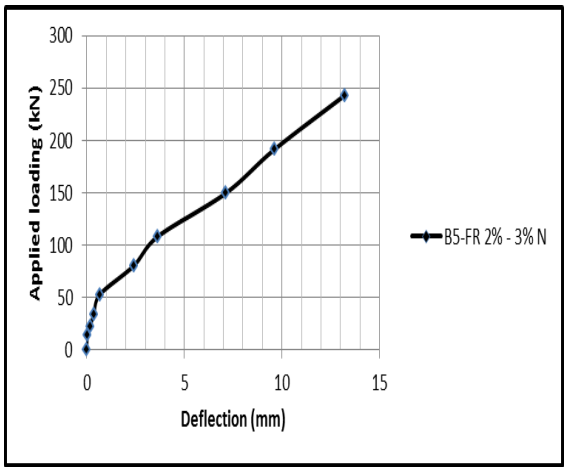

Fig. 5.31 Load – Deflection Curve of Beam (B5).

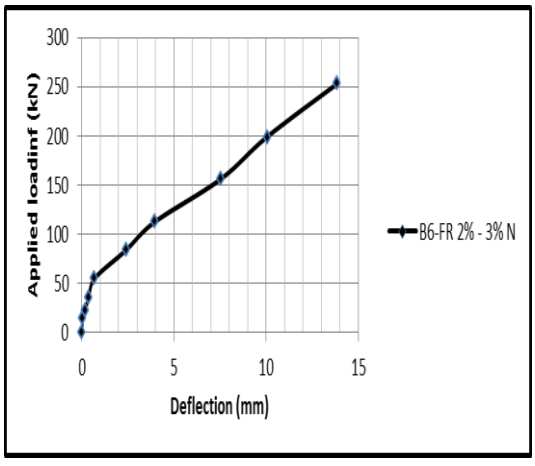

Fig. 5.32 Load – Deflection Curve of Beam (B6).

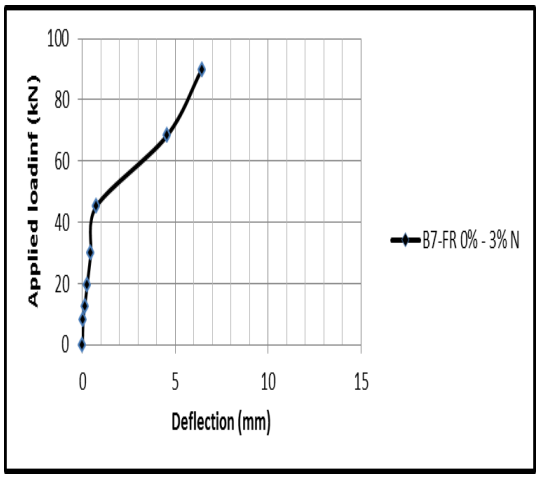

Fig. (5.33) Load – Deflection Curve of Beam (B7).

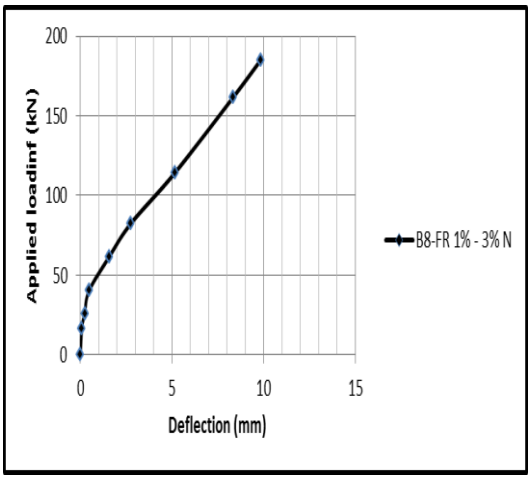

Fig. 5.34 Load – Deflection Curve of Beam (B8).

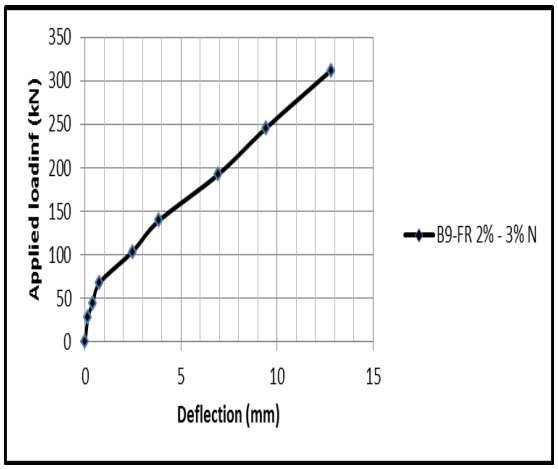

Fig. 5.35 Load – Deflection Curve of Beam (B9).

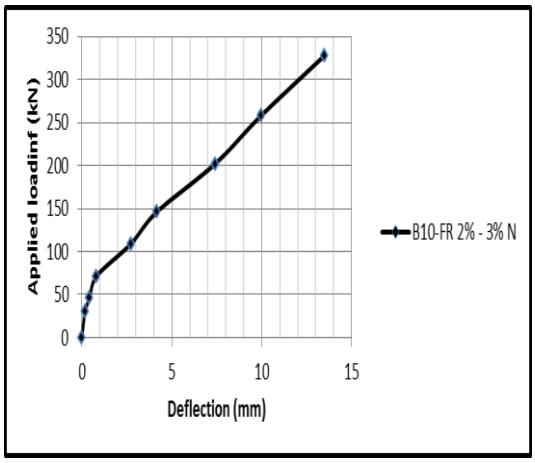

Fig. 5.36 Load – Deflection Curve of Beam (B10).

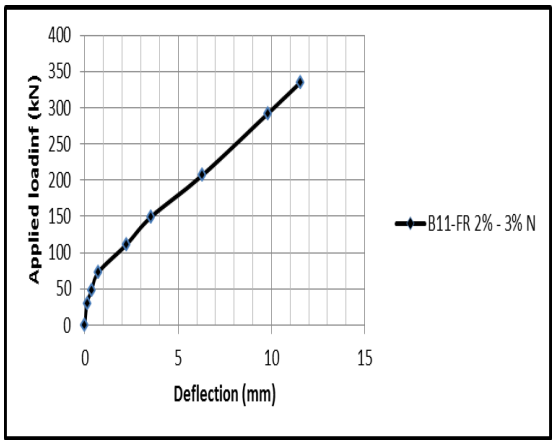

Fig. 5.37 Load – Deflection Curve of Beam (B11).

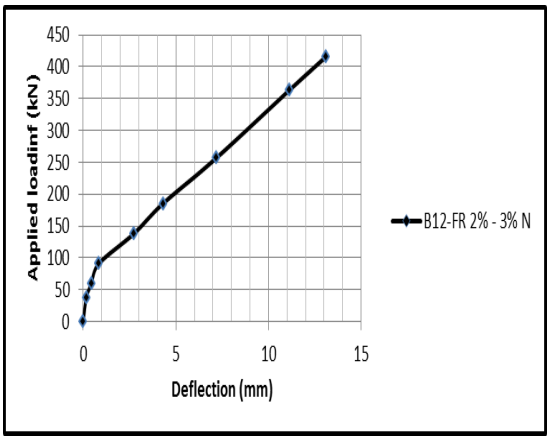

Fig. 5.38 Load – Deflection Curve of Beam (B12).

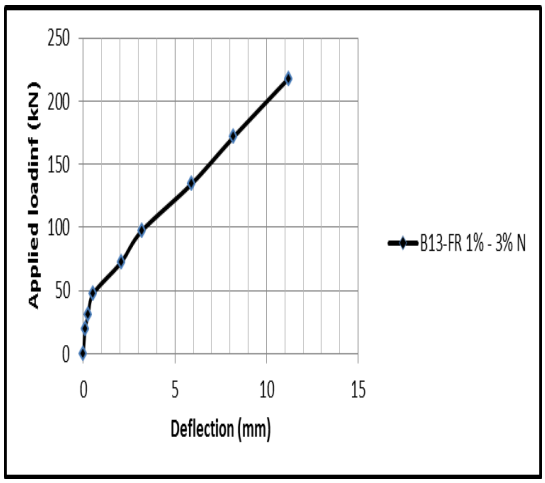

Fig. 5.39 Load – Deflection Curve of Beam (B13).

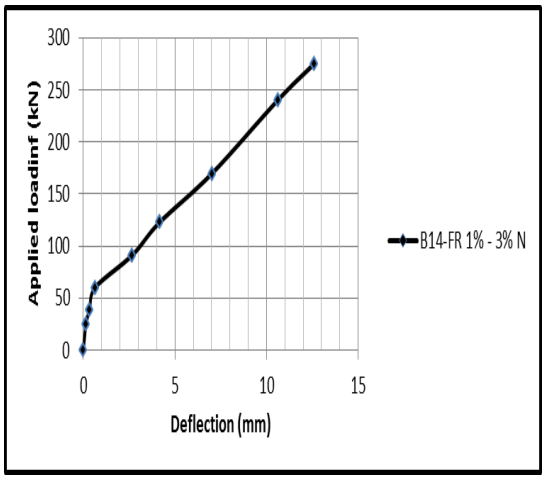

Fig. 5.40 Load – Deflection Curve of Beam (B14).

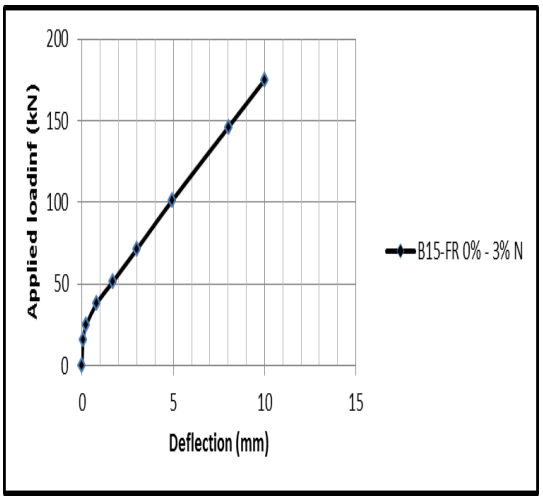

Fig. 5.41 Load – Deflection Curve of Beam (B15).

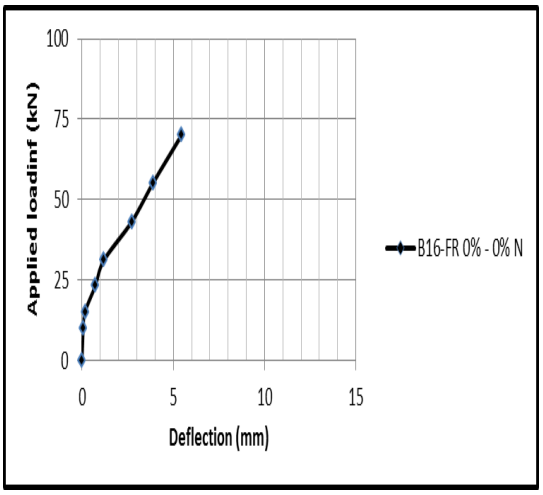

Fig. 5.42 Load – Deflection Curve of Beam (B16).

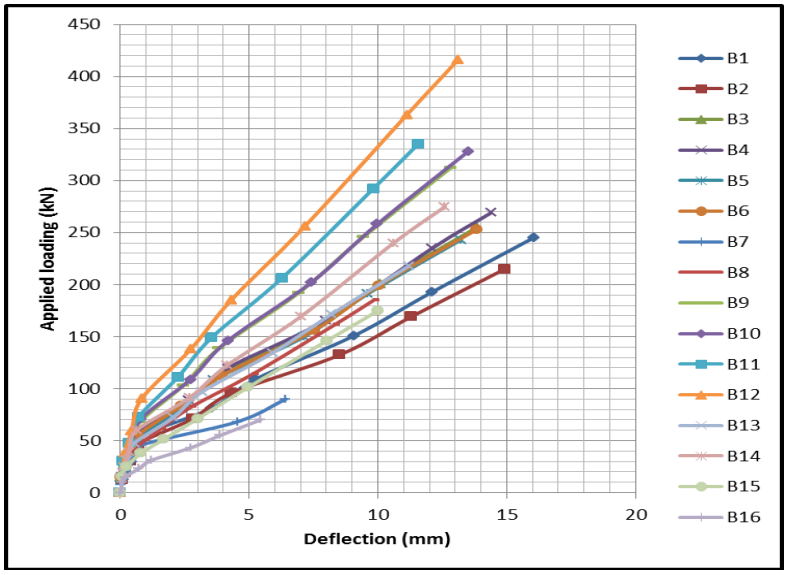

Fig. 5.43 Load – Deflection Curve for all Beams.

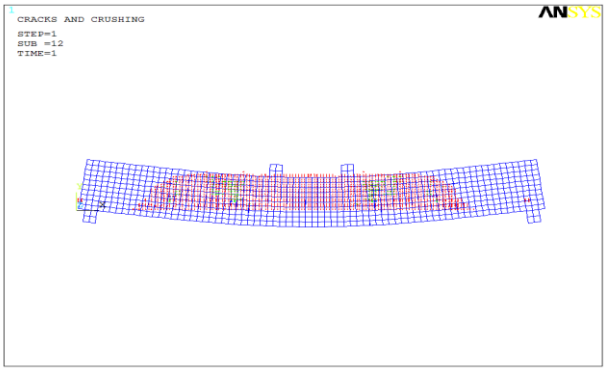

Fig. 5.44 Crack Pattern of Beam (B1) at Ultimate Load.

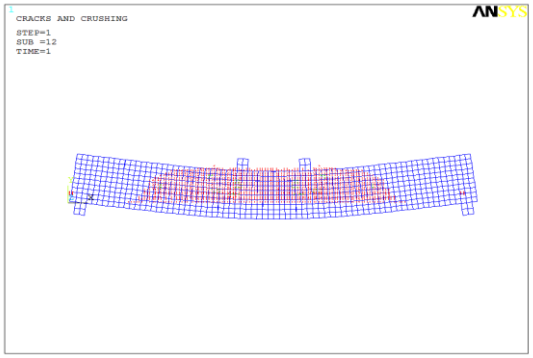

Fig. 5.45 Crack Pattern of Beam (B2) at Ultimate Load.

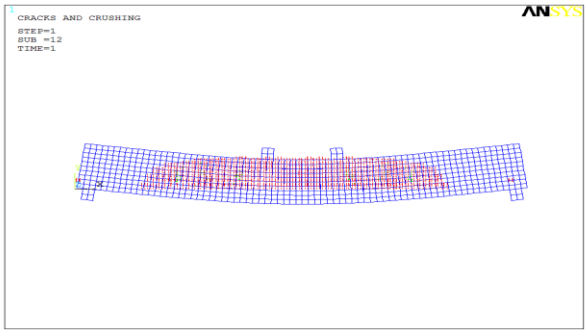

Fig. 5.46 Crack Pattern of Beam (B3) at Ultimate Load.

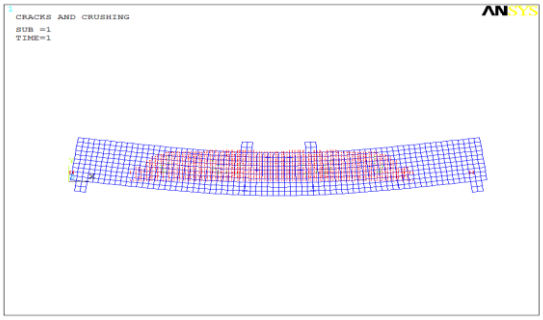

Fig. 5.47 Crack Pattern of Beam (B4) at Ultimate Load.

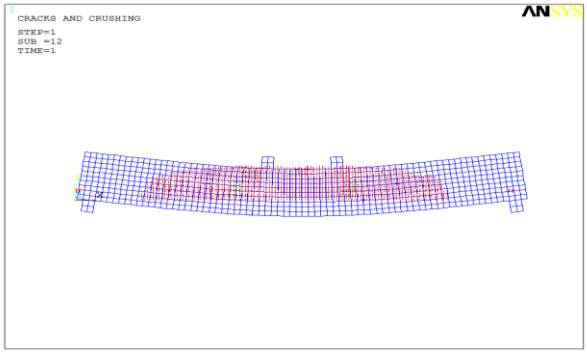

Fig. 5.48 Crack Pattern of Beam (B5) at Ultimate Load.

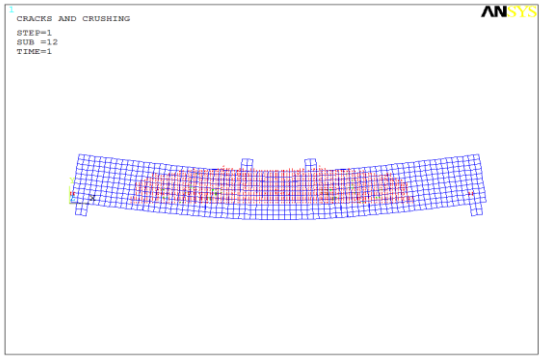

Fig. 5.49 Crack Pattern of Beam (B6) at Ultimate Load.

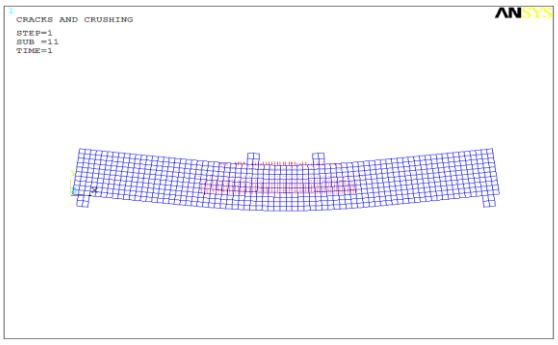

Fig. 5.50 Crack Pattern of Beam (B7) at Ultimate Load.

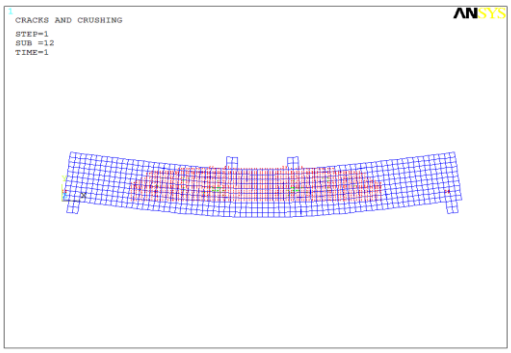

Fig. 5.51 Crack Pattern of Beam (B8) at Ultimate Load.

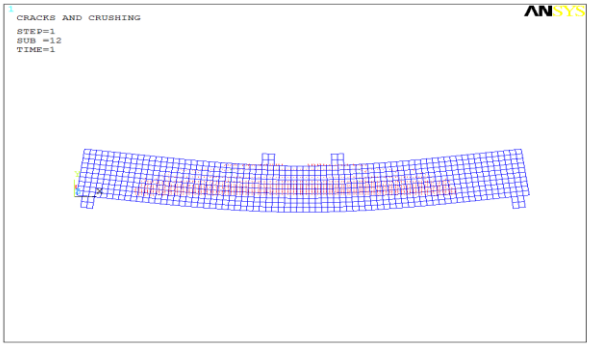

Fig. 5.52 Crack Pattern of Beam (B9) at Ultimate Load.

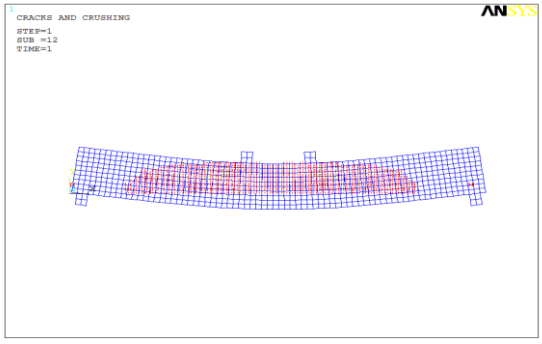

Fig. 5.53 Crack Pattern of Beam (B10) at Ultimate Load.

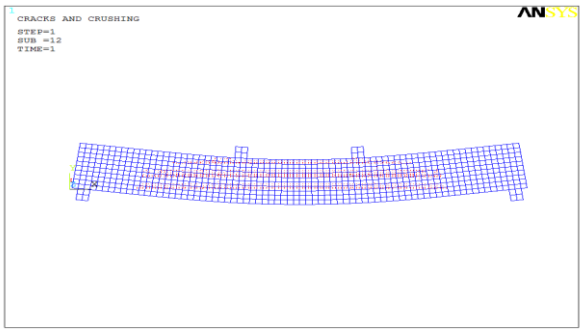

Fig. 5.54 Crack Pattern of Beam (B11) at Ultimate Load.

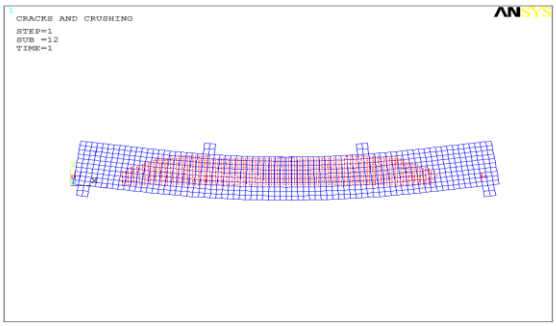

Fig. 5.55 Crack Pattern of Beam (B12) at Ultimate Load.

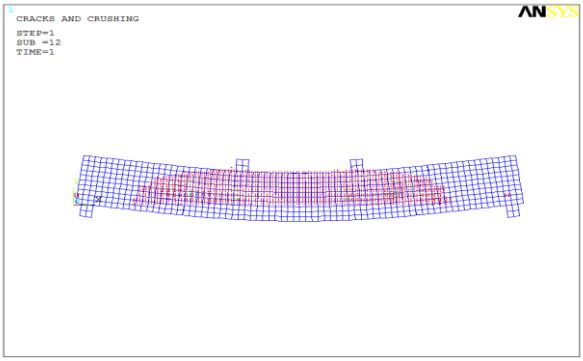

Fig. 5.56 Crack Pattern of Beam (B13) at Ultimate Load.

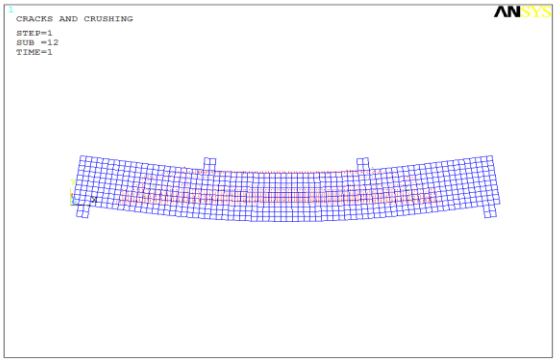

Fig. 5.57 Crack Pattern of Beam (B14) at Ultimate Load.

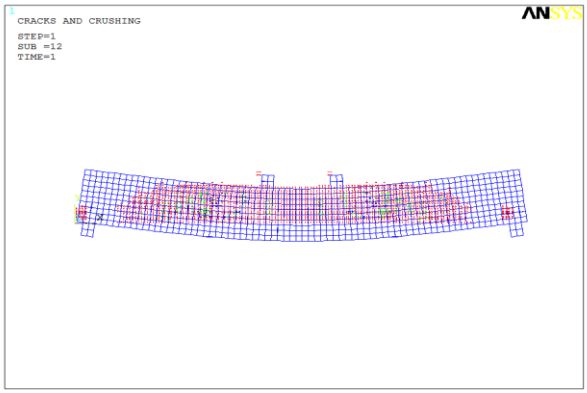

Fig. 5.58 Crack Pattern of Beam (B15) at

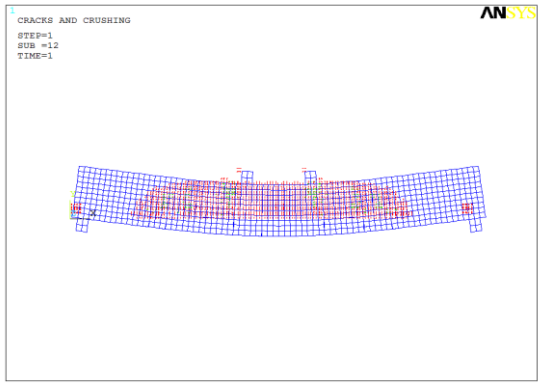

Fig. 5.59 Crack Pattern of Beam (B16) at

Ultimate Load.

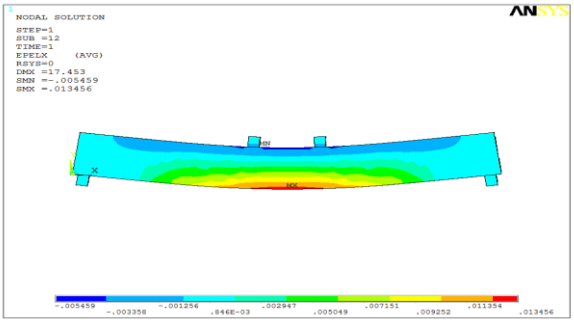

Fig. 5.60 Longitudinal Strain of Beam (B1)

Ultimate Load.

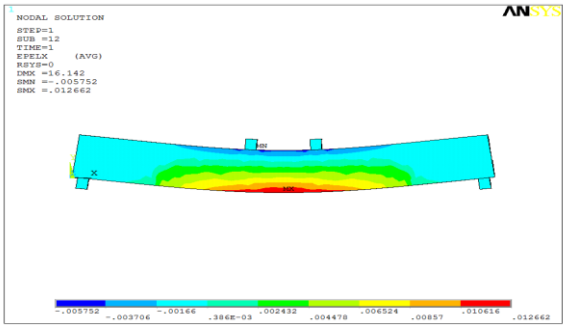

Fig. 5.61 Longitudinal Strain of Beam (B2)

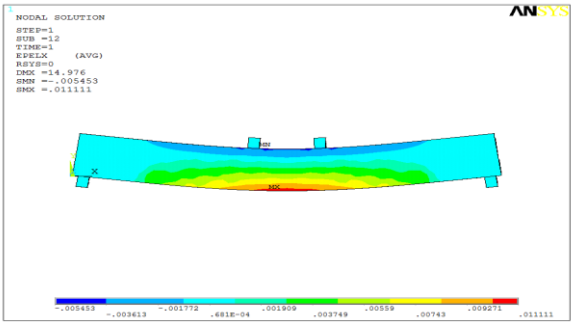

Fig. 5.62 Longitudinal Strain of Beam (B3)

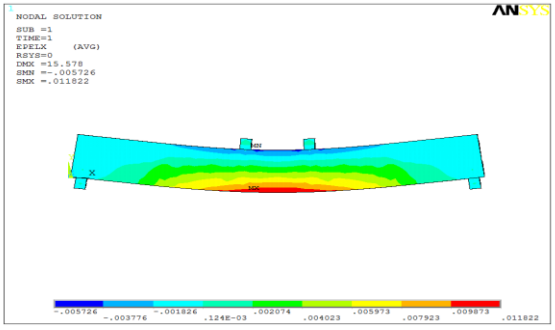

Fig. 5.63 Longitudinal Strain of Beam (B4)

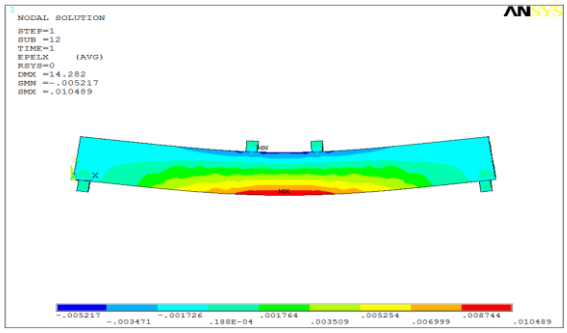

Fig. 5.64 Longitudinal Strain of Beam (B5)

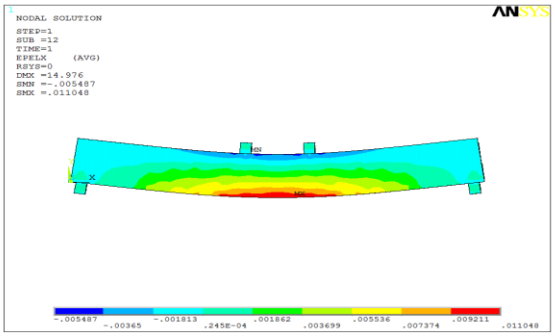

Fig. 5.65 Longitudinal Strain of Beam (B6)

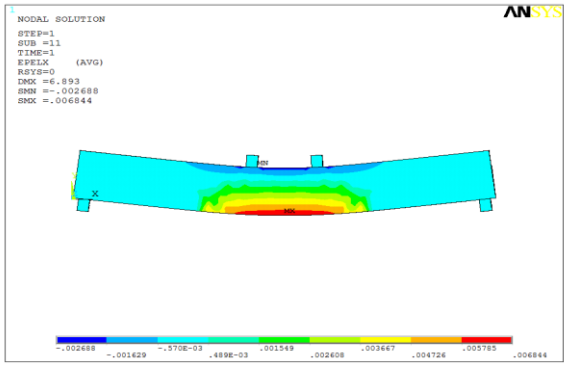

Fig. 5.66 Longitudinal Strain of Beam (B7)

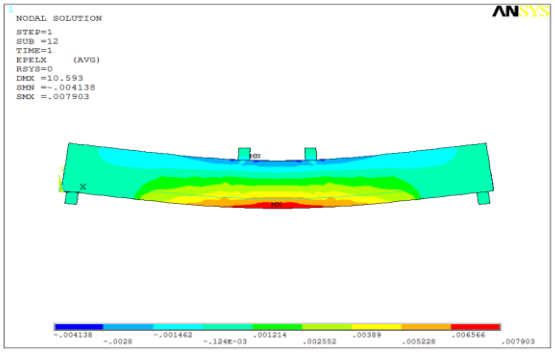

Fig. 5.67 Longitudinal Strain of Beam (B8)

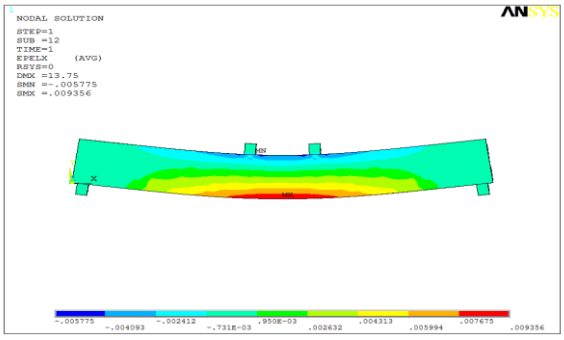

Fig. 5.68 Longitudinal Strain of Beam (B9)

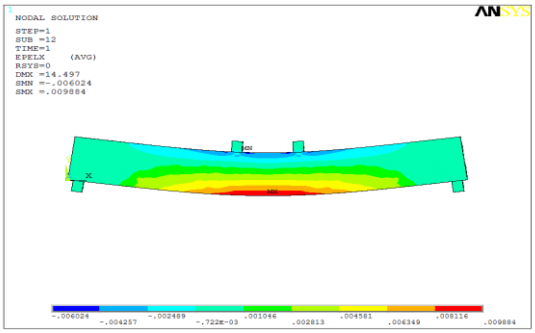

Fig. 5.69 Longitudinal Strain of Beam (B10)

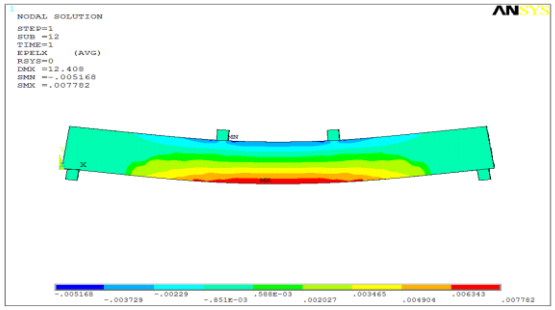

Fig. 5.70 Longitudinal Strain of Beam (B11)

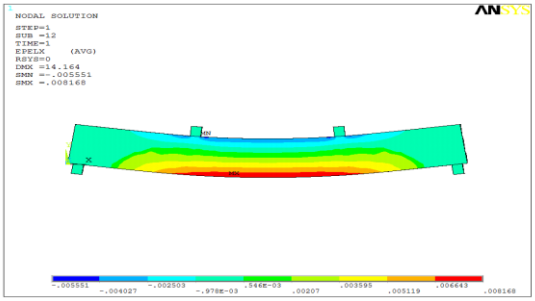

Fig. 5.71 Longitudinal Strain of Beam (B12)

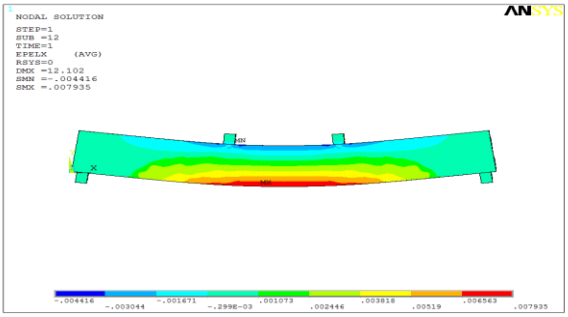

Fig. 5.72 Longitudinal Strain of Beam (B13)

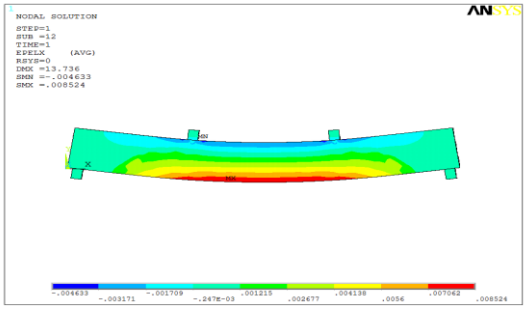

Fig. 5.73 Longitudinal Strain of Beam (B14)

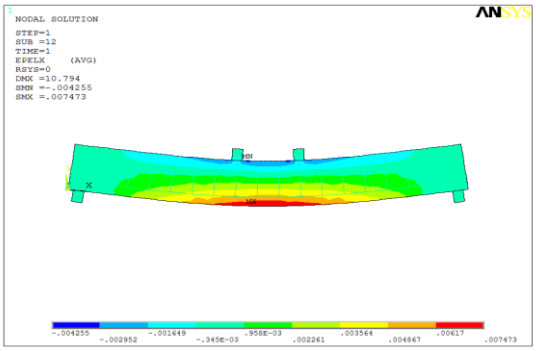

Fig. 5.74 Longitudinal Strain of Beam (B15)

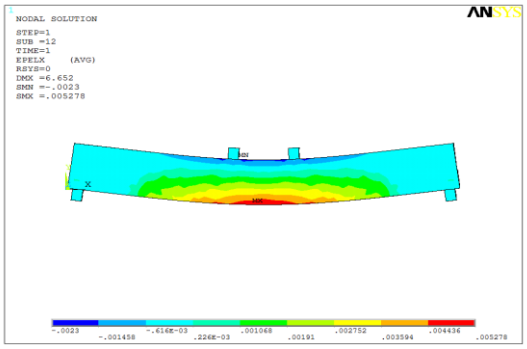

Fig. 5.75 Longitudinal Strain of Beam (B16)

5.10 Verification

Numerical analysis was adopted by ANSYS software to estimate theoretically what were obtained by the experimental tests. Figs. (5.76) to (5.91) show comparison between the experimental and theoretical load-deflection curves. From these Figures the following points can be concluded:

1. For most cases the deflection obtained by ANSYS was found greater than the experimental value at the same applied loading.
2. The general behavior of load – deflection has the same shape in all tested NSRPC beams.
3. An apparent reduction in the stiffness of a NSRPC beam can be noticed soon after the beam cracks
4. ANSYS predicts larger deflection at collapse than the experimental value.

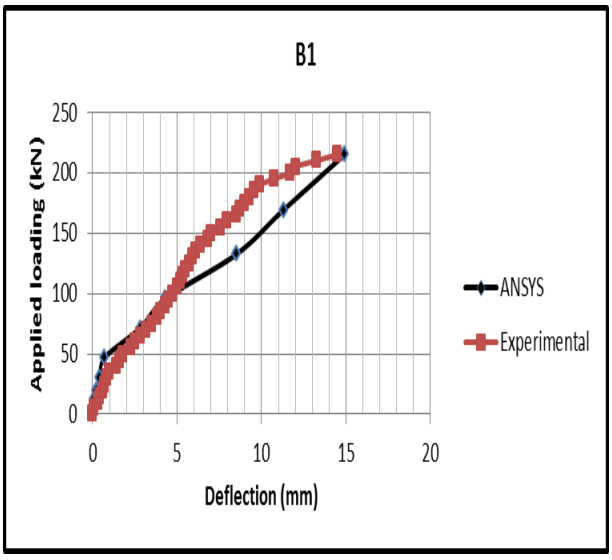

Fig. 5.76 Load – Deflection Curve of Beam (B1).

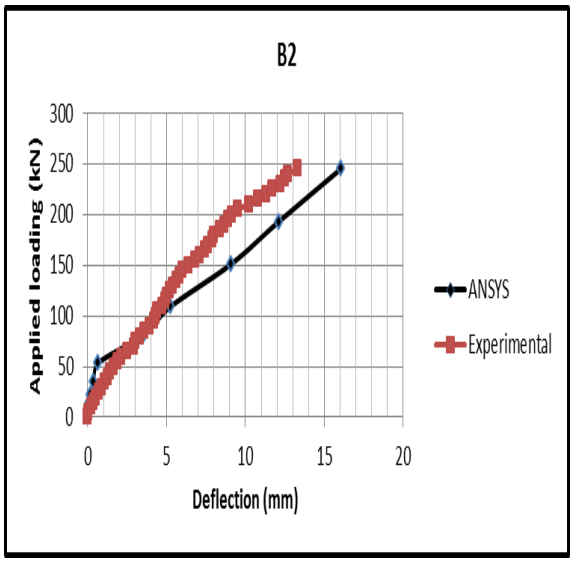

Fig. 5.77 Load – Deflection Curve of Beam (B2).

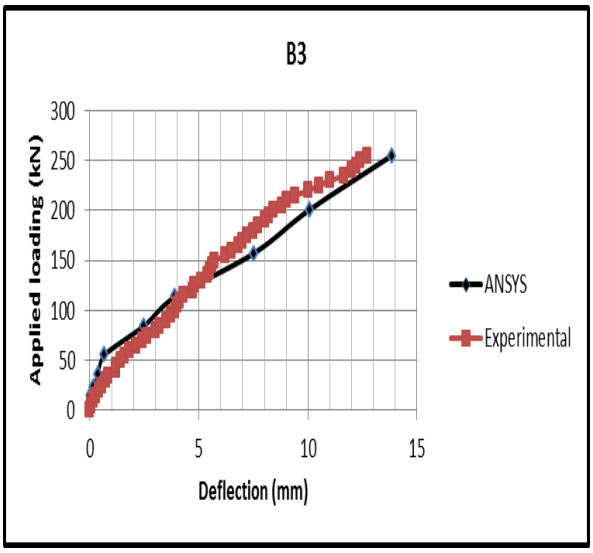

Fig. 5.78 Load – Deflection Curve of Beam (B3).

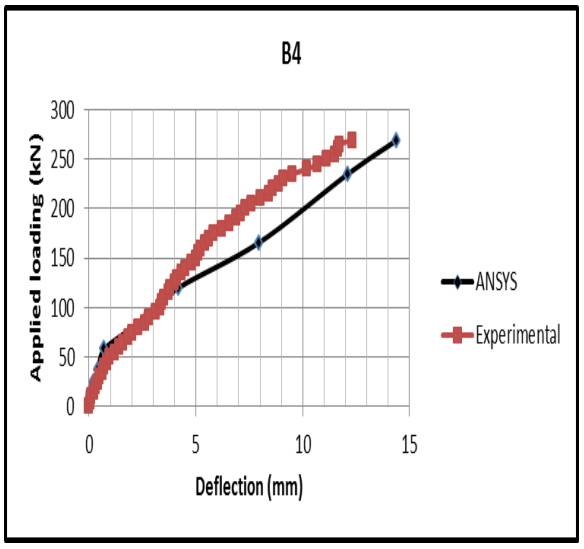

Fig. 5.79 Load – Deflection Curve of Beam (B4).

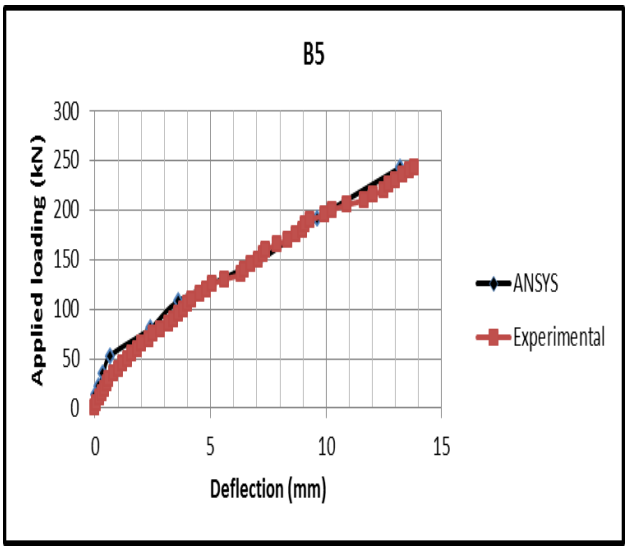

Fig. 5.80 Load – Deflection Curve of Beam (B5).

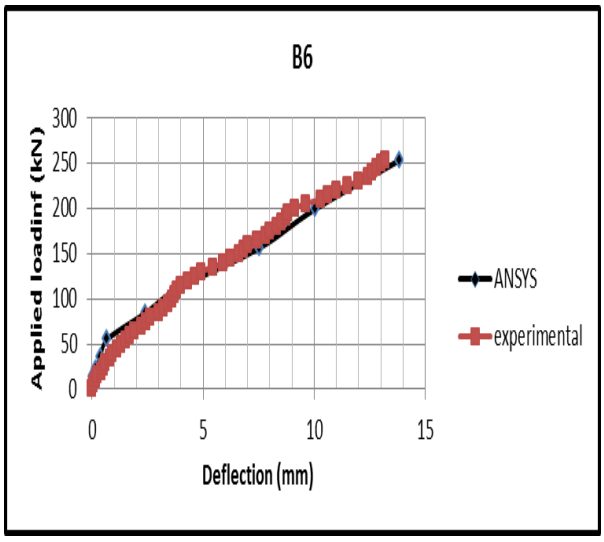

Fig. 5.81 Load – Deflection Curve of Beam (B6).

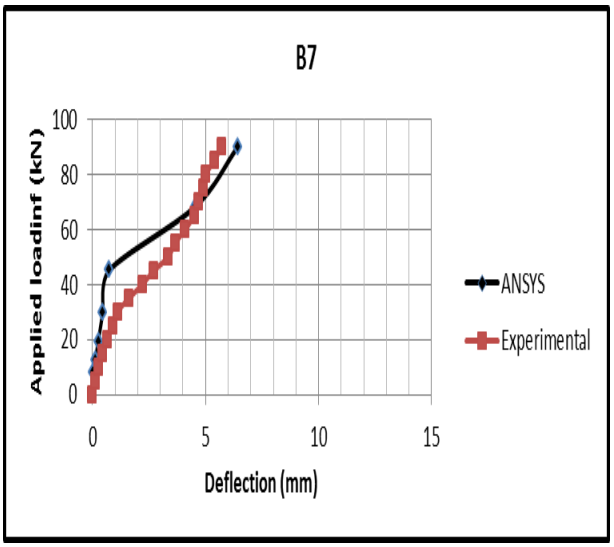

Fig. 5.82 Load – Deflection Curve of Beam (B7).

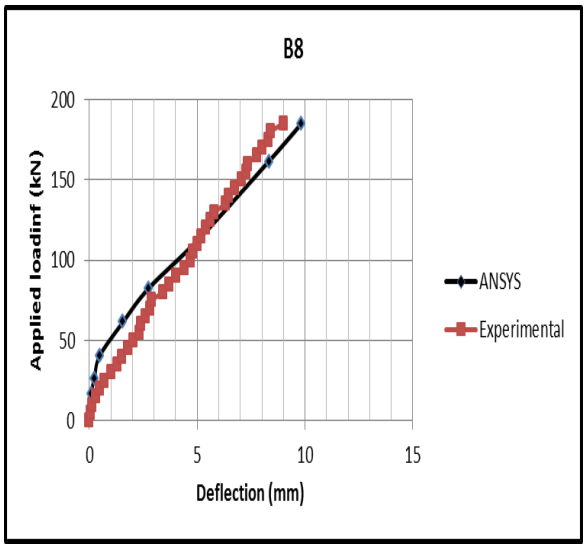

Fig. 5.83 Load – Deflection Curve of Beam (B8).

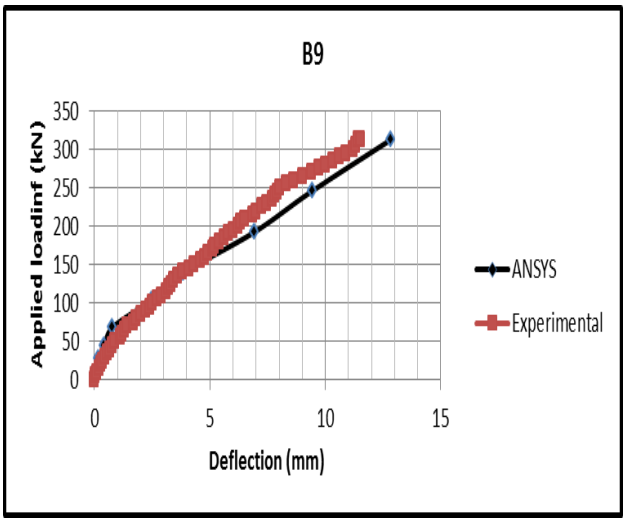

Fig. 5.84 Load – Deflection Curve of Beam (B9)

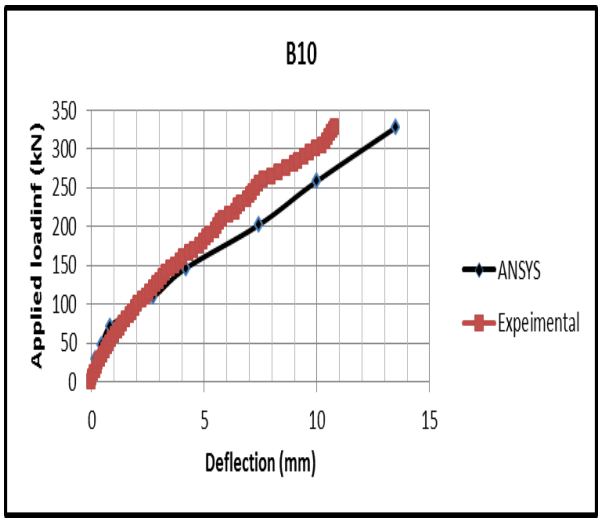

Fig. 5.85 Load – Deflection Curve of Beam (B10)

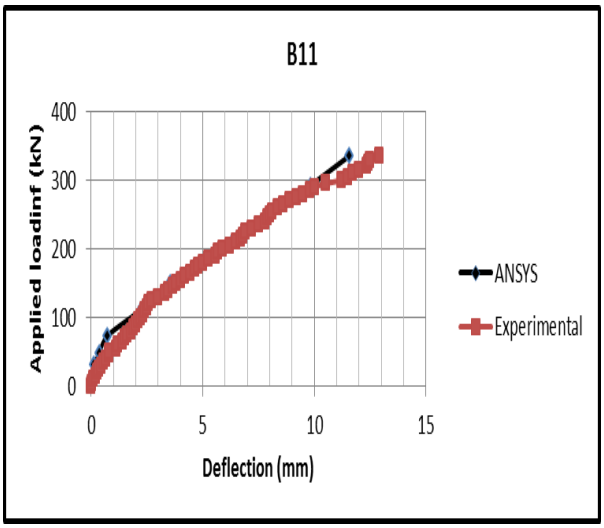

Fig. 5.86 Load – Deflection Curve of Beam (B11).

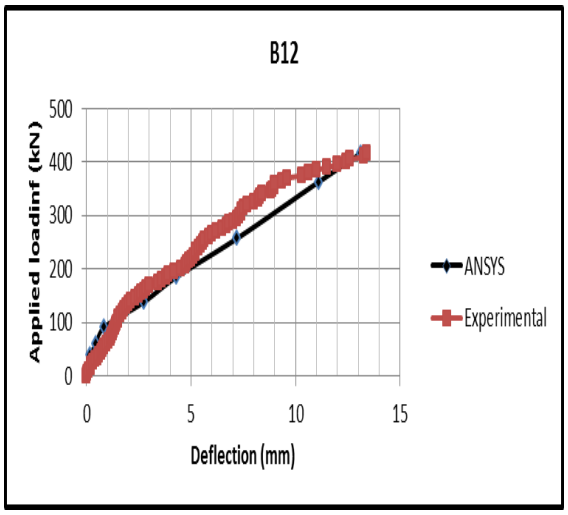

Fig. 5.87 Load – Deflection Curve of Beam (B12).

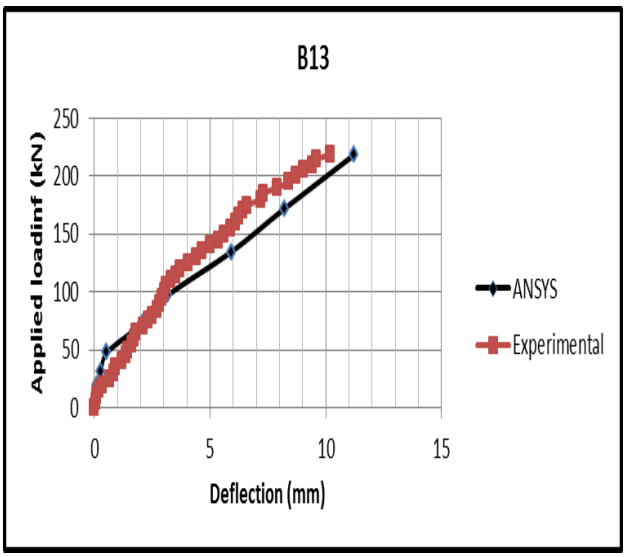

Fig. 5.88 Load – deflection Curve of Beam (B13).

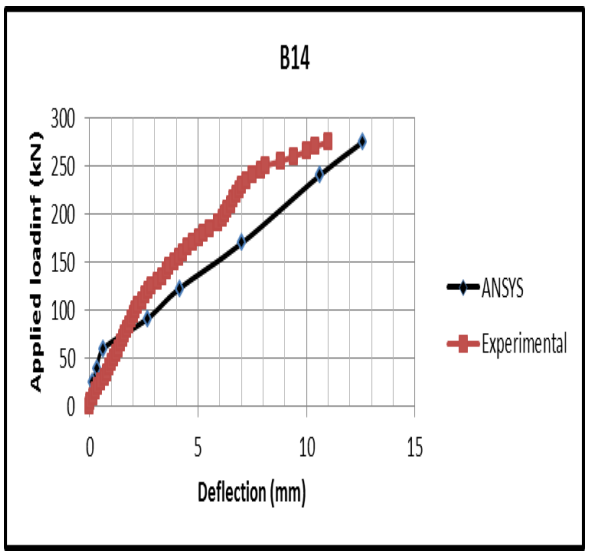

Fig. 5.89 Load – Deflection Curve of Beam (B14).

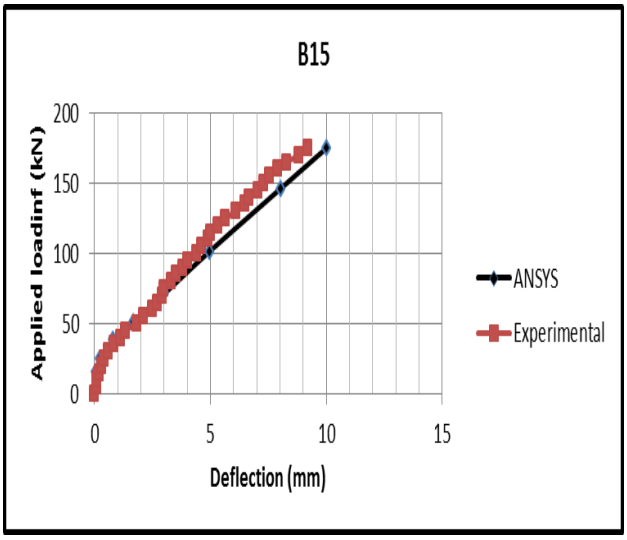

Fig. 5.90 Load – Deflection Curve of Beam (B15).

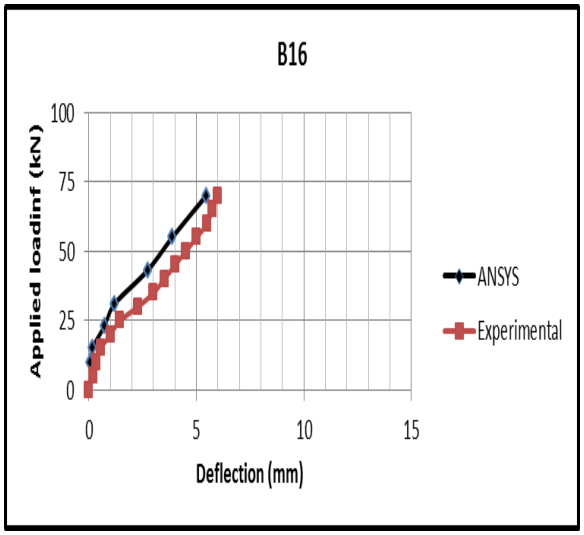

Fig. 5.91 Load – Deflection Curve of Beam (B16).